

DR. JIANKAI LIANG (Orcid ID : 0000-0002-4378-7646)

Received Date : 08-Apr-2020

Revised Date : 18-Sep-2020

Accepted Date : 10-Jul-2020

Article type : Research Article

Title: Tumors driven by *RAS* signaling harbor a natural vulnerability to oncolytic virus M1

Jing Cai¹, Kaiying Lin¹, Wei Cai¹, Yuan Lin¹, Xincheng Liu¹, Li Guo¹, Jifu Zhang², Wencang Xu², Ziqing Lin², Chun Wa Wong¹, Max Sander², Jun Hu¹, Guangmei Yan¹, Wenbo Zhu¹, Jiankai Liang^{1*}

¹Department of Pharmacology, Zhongshan School of Medicine, Sun Yat-sen University, Guangzhou 510080, China.

²Guangzhou Virotech Pharmaceutical Co., Ltd., Guangzhou 510663, China.

*Correspondence should be addressed to Jiankai Liang (liangjk5@mail.sysu.edu.cn), Department of Pharmacology, Zhongshan School of Medicine, Sun Yat-sen University, 74 Zhongshan Road II, Guangzhou 510080, China, Tel/Fax: (8620) 87330578)

This article has been accepted for publication and undergone full peer review but has not been through the copyediting, typesetting, pagination and proofreading process, which may lead to differences between this version and the [Version of Record](#). Please cite this article as [doi: 10.1002/1878-0261.12820](https://doi.org/10.1002/1878-0261.12820)

Molecular Oncology (2020) © 2020 The Authors. Published by FEBS Press and John Wiley & Sons Ltd.

This is an open access article under the terms of the Creative Commons Attribution License, which permits use, distribution and reproduction in any medium, provided the original work is properly cited.

Running title: RAS signal promotes oncolytic effect of M1 virus

Keywords: Oncolytic virus; M1; RAS; CDKN1A; Biomarker; Cancer accurate therapy

Abbreviations

CCLC	Cancer Cell Line Encyclopedia
CDK2	Cyclin-Dependent Kinase 2
Cl-casp3	Cleaved Caspase-3
dMMR	different Mismatch Repair
DNV	Newcastle Disease Virus
ER	Endoplasmic Reticulum
FDA	Food and Drug Administration
GSEA	Gene Set Enrichment Analysis
IFN	Interferon
IHC	Immunohistochemistry
IRGs	IFN-regulated genes
MOI	Multiplicity of Infection
MSI-H	Microsatellite Instability-High
NC	Negative Control
ORF	Open Reading Frame
PFU	Plaque Forming Unit
RPPA	Reversed-phase Protein Array
T-vec	Talimogene laherparepvec
STR	Short Tandem Repeat
TMA	Tissue Microarray
ZAP	Zin-finger Antiviral Protein

Abstract

Oncolytic viruses are potent anticancer agents that replicate within and kill cancer cells rather than normal cells and their selectivity is largely determined by oncogenic mutations. M1, a novel oncolytic virus strain, has been shown to target cancer cells, but the relationship between its cancer selectivity and oncogenic signaling pathways is poorly understood. Here, we report that *RAS* mutation promotes the replication and oncolytic effect of M1 in cancer, and we further provide evidence that the inhibition of the *RAS/RAF/MEK* signaling axis suppresses M1 infection and the subsequent cytopathic effects. Transcriptome analysis revealed that the inhibition of *RAS* signaling upregulates the type I interferon antiviral response, and further RNA interference screen identified *CDKN1A* as a key downstream factor that inhibits viral infection. Gain- and loss-of-function experiments confirmed that *CDKN1A* inhibited the replication and oncolytic effect of M1 virus. Subsequent TCGA data mining and tissue microarray (TMA) analysis revealed that *CDKN1A* is commonly deficient in human cancers, suggesting extensive clinical application prospects for M1. Our report indicates that viro-therapy is feasible for treating undruggable *RAS*-driven cancers and provides reliable biomarkers for personalized cancer therapy.

Introduction

Oncolytic viruses offer a new approach for cancer therapy, which exploits tumor mutations to specifically replicate within and kill tumor cells without causing harm to normal cells [1-5]. Oncolytic viruses also activate the antitumor immune response in addition to direct killing [6-8]. Since Talimogene laherparepvec (T-vec) became the first oncolytic virus approved by the US Food and Drug Administration (FDA) [9], numerous clinical trials have begun [10] and are expected to further boost the development of oncolytic therapies.

The tumor selectivity of oncolytic viruses is largely conferred by tumor-specific aberrations in signaling pathways that normally sense and block viral replication. It is now well established that cancer-specific aberrations in *BCL-2*, *WNT*, *EGFR*, *RAS*, *TP53*, *RB1*, *PTEN* and other cancer-related genes predispose cancer cells to viral infection [7, 8, 11]. For example, Newcastle Disease Virus (DNV) targets cancer cells overexpressing *BCL-XL*, which prevents apoptosis and thereby permits the virus to utilize the transcription and translation machinery for the synthesis of the viral nucleocapsid [12]. The activation of *WNT* signaling, a key pathway in embryonic development that directs cell proliferation, polarity and developmental fate, has been found to attenuate the host antiviral response and facilitate the infection and replication of several kinds of viruses [13-15]. In addition, cancer cells with *RAS* mutations cannot activate the PKR pathway which functions to prevent the production and spread of virus, rendering cancer cells permissive to reovirus, herpesvirus and vaccinia virus infection [16-19].

M1 virus is an enveloped alphavirus with an 11.7 kb positive single-stranded RNA genome [20], which contains four nonstructural proteins and five structural proteins. Our previous studies demonstrated that M1 is a potent oncolytic virus that selectively targets and induces irreversible endoplasmic reticulum (ER) stress-mediated apoptosis in different cancers *in vitro* and *in vivo* [21-23]. More interestingly, the oncolytic effect of M1 can be enhanced by small-molecule compounds, including *BCL-XL* inhibitors, Smac mimetics,

and DNA-PK inhibitors [24-29]. Our previous study established that M1 virus is a promising oncolytic virus for clinical cancer therapy. Though we have identified that the deficiency of zinc-finger antiviral protein (ZAP) mediates the cancer selectivity of M1, however, the relationship between the cancer selectivity of M1 virus and oncogenic signals has not yet been illuminated.

In this study, we analyzed the relationship between viral infection and oncogenic mutations in 52 tumor cell lines and found that among the mutations in these cell lines, *K-RAS* aberration promotes viral infection. Further expression profiling identified CDKN1A as a key factor downstream of the RAS/RAF/MEK signaling pathway that inhibits the replication of M1 virus. The knockdown of CDKN1A enhances the oncolytic effect of M1 virus in nude mice bearing human tumor cells, which largely represents the characteristics of human cancer. This study identifies *RAS* mutation and deficiency of CDKN1A as candidate biomarkers for personalized anticancer viro-therapy.

Methods

Cell culture and M1 viruses.

All cell lines were purchased from the American Type Culture Collection (ATCC, Manassas, VA, US). Cells were cultured in DMEM supplemented with 10% (vol/vol) FBS (Thermo Fisher Scientific) and 1% penicillin/streptomycin (Thermo Fisher Scientific, Waltham, MA, US). All cell lines were cultured at 37°C in a 5% CO₂ environment. All cell lines were authenticated by the short tandem repeat (STR) assay and were mycoplasma free according to the MycoGuard mycoplasma PCR detection kit (MPD-T-050, GeneCopoeia, Rockville, MD, US).

The M1 virus was grown in the Vero cell line and collected for experiments. The M1-c6v1 strain of virus was provided by Guangzhou Virotech Pharmaceutical Co., Ltd. M1-GFP is a recombinant M1 engineered to express jellyfish green fluorescent protein [28]. The viral

titer was determined by the TCID50 method using the BHK-21 cell line and converted to plaque forming unit (PFU).

Lentiviruses and infections

Lentiviruses containing the CDKN1A (Gene ID: 1026) open reading frame (ORF) (LPP-G0313-Lv242-100) and shRNA (pLKD-CMV-mcherry-2A-Puro-U6-CDKN1A shRNA) of CDKN1A were constructed and packaged by GeneCopoeia (Rockville, MD, US) and OBiO Technology, Shanghai China. The HCT-15 cell line was transfected with lentiviruses containing 5 µg/ml polybrene (Sigma-Aldrich, St. Louis, MO, US); the multiplicity of infection (MOI) was 1. Three days after viral transfection, cells were selected with 1 µg/ml puromycin for 7-14 days to establish a CDKN1A stably expressing cell line.

Cell viability assay

Cells were seeded in 96-well plates at 3,000 cells per well. After different treatments indicated in the figure legends were administered, 3-(4,5-dimethylthiazol-2-yl)-2,5-diphenyltetrazolium bromide (MTT) was added (1 mg/ml) and incubated at 37°C for 3 hours. The supernatants were removed, and the MTT precipitate was dissolved in 100 µl of DMSO. The optical absorbance was determined at 570 nm by a microplate reader (synergy H1, Gene Company, Hong Kong, China).

Antibodies and reagents

The following antibodies and reagents were used in this study: ERK (#4695, Cell Signaling Technology, Danvers, MA, US, RRID: AB_390779); p-ERK (#4370, Cell Signaling Technology, RRID: AB_2315112); CDKN1A (#2947, Cell Signaling Technology, RRID: AB_823586); Ki-67 (#9449, Cell Signaling Technology, RRID: AB_2797703); Cleaved caspase 3 (#9664, Cell Signaling Technology, RRID: AB_2070042); E1 and NS3 (Beijing Protein Innovation, Beijing, China); sorafenib (#S7397, Selleckchem, Houston, TX, US); U0126 (#S1102, Selleckchem); Cobimetinib (#S8041, Selleckchem); Trametinib (S2673,

Selleckchem); K03861 (#S8100, Selleckchem); and polybrene (Sigma-Aldrich); puromycin (Thermo Fisher Scientific).

Expression profiling

HCT 15 tumor cells were treated with control, M1 (MOI=1 pfu/cell), U0126 (16 μ M) or M1 (MOI=1 pfu/cell) plus U0126 (16 μ M) for 24 hours. Total RNA was extracted from 1×10^6 cells with TRIzol Reagent (Thermo Fisher Scientific) and was sent to CapitalBio (Beijing, China) for labeling and hybridization on the Affymetrix GeneChip Human Genome U133 Plus 2.0 Array.

RNA interference

siRNAs specific to different genes and control nontargeting siRNA were synthesized by Sigma-Aldrich. The cells were transfected with the siRNAs (50 nM) using Lipofectamine RNAiMAX (Thermo Fisher Scientific) in Opti-MEM medium (Thermo Fisher Scientific).

The sequences of the siRNAs are listed below.

si-CDKN1A 001: 5'-TGATCTTCTCCAAGAGGAA-3'

si-CDKN1A 002: 5'-GAATGAGAGGTTCCCTAAGA-3'

si-CDKN1A 003: 5'-TGGCGGGCTGCATCCAGGA-3'

si-IFIT3 001: 5'-GACGGAATGTTATCAGACA-3'

si-IFIT3 002: 5'-GGATAATCACCCAGAGAAA-3'

si-IFIT3 003: 5'-CCAGAGAGCTCCTCTCTAA-3'

si-IFI27 001: 5'-CTCTCCGGATTGACCAAGT-3'

si-IFI27 002: 5'-CTGTCATTGCGAGGTTCTA-3'

si-IFI27 003: 5'-CCAGGATTGCTACAGTTGT-3'

si-MX2 001: 5'-GCACGATTGAAGACATAAA-3'

si-MX2 002: 5'-GGGACGCCTTCACAGAATA-3'

si-MX2 003: 5'-GGAGAATGAGACCCGTTTA-3'

si-ID1 001: 5'-GAACTCGGAATCCGAAGTT-3'

si-ID1 002: 5'-CACGTCATCGACTACATCA-3'

si-ID1 003: 5'-TCAGGGACCTTCAGTTGGA-3'

RT-qPCR

Total RNA was extracted using TRIzol (Thermo Fisher Scientific), and 2 µg of total RNA was reverse-transcribed to cDNA with oligo (dT) (synthesized by Thermo Fisher Scientific) and RevertAid Reverse Transcriptase (Thermo Fisher Scientific). The expression levels of the specific genes were calculated by the comparative Ct method using SuperReal PreMix SYBR Green (FP204-02, TIANGEN, Beijing, China) and an Applied Biosystem 7500 Fast Real-Time PCR system (Thermo Fisher Scientific, RRID: SCR_014596). The sequences of the primers are listed below.

ID1 Forward: 5'-CTGCTCTACGACATGAACGG-3'

ID1 Reverse: 5'-GAAGGTCCCTGATGTAGTCGAT-3'

DDIT4 Forward: 5'-TGAGGATGAACACTTGTGTGC-3'

DDIT4 Reverse: 5'-CCAACCTGGCTAGGCATCAGC-3'

CYP1B1 Forward: 5'-AAGTTCTTGAGGCACTGCGAA-3'

CYP1B1 Reverse: 5'-GGCCGGTACGTTCTCCAAAT-3'

IFI27 Forward: 5'-TGCTCTCACCTCATCAGCAGT-3'

IFI27 Reverse: 5'-CACAACCTCCTCCAATCACAAC-3'

CDKN1A Forward: 5'-CGATGGAACTTCGACTTTGTCA-3'

CDKN1A Reverse: 5'-GCACAAGGGTACAAGACAGTG-3'

MX2 Forward: 5'-CAGAGGCAGCGGAATCGTAA-3'

MX2 Reverse: 5'-TGAAGCTCTAGCTCGGTGTTC-3'

ATP10D Forward: 5'-GTGGTGGTCCTTACAATTATCGC-3'

ATP10D Reverse: 5'-CCCAACAGTAACGTCTTTCCAG-3'

PNRC1 Forward: 5'-ACTTGCCACTAACCAAGATCAC-3'

PNRC1 Reverse: 5'-TTGGAAGAACAACACTAGGAGAAGGT-3'

JUN Forward: 5'-AACAGGTGGCACAGCTTAAAC-3'

JUN Reverse: 5'-CAACTGCTGCGTTAGCATGAG-3'

Western blot analysis

Cell samples were prepared using M-PER Mammalian Protein Extraction Reagent (Thermo Fisher Scientific) and then separated by sodium dodecyl sulfate-polyacrylamide gel electrophoresis. The membranes were visualized with a ChemiDoc XRS+ System (Bio-Rad, Hercules, CA, US) using Immobilon Western Chemiluminescent HRP Substrate (Millipore, Darmstadt, Germany).

Animal models

The mouse study was approved by the Animal Ethics and Welfare Committee of Sun Yat-sen University, and all experiments were conducted according to the US "Public Health Service Policy on Humane Care and Use of Laboratory Animals". HCT-15-NC and HCT-15-shCDKN1A (5×10^6 cells/mouse) tumor cells were implanted subcutaneously into the hind flanks of 5-week-old 16 g female BALB/c-nu/nu mice (the mice were bought from Nanjing Biomedical Research Institute, China, and housed in an SPF facility with normal temperature and food). After 6 days, tumors were observed (approximately 50 mm³). M1 virus (3.48×10^8 TCID₅₀ per mouse) was injected intravenously for 14 days. The lengths and widths of the tumors were measured every 3 days, and the tumor volume was calculated according to the formula $(\text{length} \times \text{width}^2)/2$. At the termination of the experiment, all mice were euthanized by overdose anesthesia, and the tumors were removed and fixed in 4% paraformaldehyde for subsequent immunohistochemistry (IHC) assays. The study was randomized and blind.

For detection of M1 viral copy number in tumor tissues, 3 days after the first medication, 3 mice in M1 virus treated HCT-15-NC and HCT-15-shCDKN1A tumor groups were euthanized by overdose anesthesia, and tumors were stripped out. Total RNA in tumors was extracted by Eastep[®] Super total RNA extraction kit (Promega), Viral copy numbers were detected by Taqman qRT-PCR with FastKing One Step RT-qPCR Kit (TIANGEN)

according to the manufacturer's instructions. The sequence of primers and probe were listed as below:

Forward primer: 5'-GGGATTCACCTACACCTGCTTAGAC-3'

Reverse primer: 5'-GCTGACTCTGTCTGCGTAACC-3'

Prober: 5'-CTCTCATCAGCAGCGAGCCTCCT-3'

Immunohistochemistry (IHC) assay.

The expression of Ki-67 and cleaved caspase 3 in the tumors was assessed by immunohistochemistry (IHC). Briefly, tumor sections were dewaxed in xylene, hydrated in decreasing concentrations of ethanol, immersed in 0.3% H₂O₂-methanol for 30 minutes, washed with phosphate-buffered saline, and probed with monoclonal antibodies or isotype controls at 4°C overnight. After being washed, the sections were incubated with biotinylated goat anti-rabbit or anti-mouse IgG at room temperature for 2 hours. Immunostaining was visualized with streptavidin/peroxidase complex and diaminobenzidine, and sections were counterstained with hematoxylin.

Tissue microarray (TMA)

TMA's were purchased from Shanghai Biochip China. IHC staining was performed on 5 µm sections of the TMA's with CDKN1A antibody (#2947, Cell Signaling Technology, RRID: AB_823586). TMA slides were scanned using an Aperio slide scanner, and the staining intensity of CDKN1A was analyzed by Aperio ImageScope software (ImageScope, RRID: SCR_014311).

Statistics

All statistical analyses were performed using GraphPad Prism software 8.0 (RRID: SCR_002798) and SPSS 18.0 software (RRID: SCR_002865). Most of the data were analyzed by a two-tailed Student's t test or one-way ANOVA with Dunnett's test for pairwise comparisons. Tumor volumes were analyzed by a two-tailed paired Student's t

test. Correlations were analyzed by the Pearson's test. The expression of CDKN1A in paired cancer and adjacent non-neoplastic tissue was analyzed by a two-tailed paired Student's t test. Phase contrast and fluorescence pictures were taken with a Nikon Eclipse A1 microscope. The IHC staining intensity was analyzed by ImageScope software (ImageScope, RRID: SCR_014311). The Wilcoxon signed-rank test was used to compare paired non-normally distributed data. Bars show the mean \pm SD or SEM of three independent repeated experiments. Significant differences were accepted if the *p*-value was < 0.05 .

Results

Tumor cell lines harboring *K-RAS* mutation are more sensitive to M1 virus than those without *K-RAS* mutation

To investigate the relationship between the selectivity of M1 virus and oncogenic signals in tumors, we analyzed the relationship between the oncolytic effect (represented by values of EC50) of M1 virus (Supplementary Table S1) and cellular oncogenic mutations in 52 tumor cell lines originating from various types of tissue. The oncogenic mutation data were retrieved from the Cancer Cell Line Encyclopedia (CCLE) database [30], and all of the mutations in the 52 cell lines are listed in Supplementary Table S2. By analyzing the EC50 values of M1 virus in these cell lines with or without oncogenic mutations, we found that the *K-RAS*, *MDN1*, *RYR3* and *PIEZO2* genes are frequently mutated in the cell lines with higher sensitivity to M1 virus (Figure 1A). Of the genes listed, *K-RAS* is the most notable and undruggable target, and further statistical analysis confirmed that M1 virus showed lower EC50 values which represent better antitumor effects in the cell lines with *K-RAS* mutation than those with wild type *K-RAS* (Figure 1B and Supplementary Table S1).

To test whether mutant *K-RAS* indeed affect the sensitivity of cancer cells to M1 virus, specific si-RNAs to *K-RAS* were used to knock down the expression of *K-RAS* in HCT-15

and MIA PaCa-2 cell lines (Supplementary Figure S1), which harbor the mutant *K-RAS* (indicated in supplementary Table S1). In these cell lines, knock down of *K-RAS* inhibited the cell killing by M1 virus (Figure 1C-1D), suppressed the infection rate of M1 virus as shown by flow cytometry and fluorescence imaging (Figure 1E-1G). Moreover, knock down of *K-RAS* inhibited the replication of M1 virus as shown by viral titer detected by TCID50 method (Figure 1H-1I). Taken together, the results suggest that *K-RAS* mutation promotes the replication and subsequent oncolytic effect of M1 virus.

RAS/RAF/MEK signaling inhibitors suppress the oncolytic efficiency and gene expression of M1 virus

RAS mutation results in the activation of the RAS/RAF/MEK pathway, so we investigated whether inhibitors of the RAS/RAF/MEK pathway affect the oncolytic efficiency and gene expression of M1 virus in tumor cells. Sorafenib is an approved drug for the treatment of different types of cancer that has been reported to preferably inhibit the activity of RAF [31], while U0126 selectively inhibits MEK1/2 [32]. In the pancreatic carcinoma cell line MIA PaCa-2 and colorectal carcinoma cell line HCT-15, both sorafenib and U0126 modestly but significantly inhibited the oncolytic effect of M1 (Figure 2A-2D). Cobimetinib and trametinib, two other MEK inhibitors approved by the FDA, also modestly but significantly inhibited the oncolytic effect of M1 virus (Supplementary Figure S2A-S2D). We previously reported that the cancer targeting and killing properties of M1 virus depend on the replication of the virus in cancer cells [23], so we used M1 virus engineered to express the reporter protein GFP (M1-GFP) to trace the gene expression of the virus in tumor cells. Phase contrast and fluorescence imaging showed that U0126 suppressed the reporter gene expression and M1-induced cytopathic effects (Figure 2E-2F). Cytometry analysis consistently proved that the M1 virus infection rate was modestly but significantly inhibited by U0126 treatment (Figure 2G-2H). Furthermore, the expression of viral proteins E1 and NS3 decreased significantly following U0126 treatment, which effectively inhibited the phosphorylation of ERK (Figure 2I-2J). In conclusion, RAS/RAF/MEK

signaling promotes the oncolytic effect of M1 virus by upregulating viral gene expression, which suggests the acceleration of viral replication.

Inhibition of the RAS/RAF/MEK pathway upregulates the expression of antiviral signaling pathway members

To identify the mechanism by which RAS/RAF/MEK signaling promotes the replication of M1, gene expression profiling was performed in the HCT-15 cell line under vehicle, U0126, M1 or M1 plus U0126 treatment conditions. Gene Set Enrichment Analysis (GSEA) proved that U0126 effectively downregulated the RAS signaling pathway (Figure 3A and Supplementary Table S3). It is well known that the promotion of viral replication by oncogenic signals is due to crosstalk of them with antiviral pathways, which consist mainly of interferon (IFN) signaling [7]. Among the three classes of interferons (IFNs), type I IFNs are known to be essential for mounting a robust host response against viral infection [33]. We hypothesized that U0126 might upregulate antiviral interferon pathway activity to inhibit the replication and oncolytic effect of M1 virus.

GSEA revealed that U0126 strongly upregulated the IFN- α and IFN- β response pathways after M1 virus infection (Figure 3B-3C and Supplementary Table S4-S5). To identify the key factors upregulated by U0126 to inhibit the replication and oncolytic effect of M1 virus, we focused on the expression of 317 IFN-regulated genes (IRGs), which were identified to be crucial antiviral effectors for alphavirus M1 [23]. The heatmap of the top 20 IRGs upregulated by U0126 plus M1 compared with M1 (MU/M) is shown in Figure 3D. In addition, qPCR was used to verify the expression of the top 10 IRGs in HCT-15 cell line. We found that the expression of *IFIT3*, *CDKN1A*, *MX2*, *IFI27* and *ID1* was significantly increased in the M1 plus U0126 group compared with the M1 treatment group (Figure 3E-3F). When we ranked the fold change between the M1 plus U0126 group and the M1 group (MU/M), these five genes comprised the top five (Figure 3G). Taken together, these results indicate that the inhibition of RAS signaling by U0126 upregulates the

interferon-mediated innate immune response of cancer cells, which may result in the attenuation of the replication and oncolytic effect of M1 virus.

CDKN1A is a key antiviral factor downstream of RAS signaling that inhibits the replication of M1 virus.

To further identify the specific IRG that inhibits M1 viral infection, we used siRNAs to knock down the five genes identified above in the HCT-15 cell line, including *CDKN1A*, *IFI27*, *IFIT3*, *MX2* and *ID1*. The siRNA effectively knocked down the expression of these genes (Supplementary Figure S3), and only the knockdown of *CDKN1A* significantly increased the infection of M1 virus (Figure 4A), indicating that *CDKN1A* might be a key factor. *CDKN1A*, also known as p21, is a universal cell cycle inhibitor directly controlled by p53 and p53-independent pathways [34]. To further elucidate the antiviral function of *CDKN1A*, we knocked down the expression of *CDKN1A* in two more pancreatic carcinoma cell lines, MIA PaCa-2 and PANC-1 (Figure 4B). Knocking down *CDKN1A* increased both the M1 infection and viral titer in these cell lines (Figure 4C-4F). Further knockout of *CDKN1A* in HCT-15 and PANC-1 cell lines by shRNA also increased the infection and titer of M1 virus (Figure 4G-4I). Further, the lentivirus-mediated overexpression of *CDKN1A* notably reduced the M1 virus infection and titer (Figure 4J-4K). Moreover, the overexpression of *CDKN1A* in SW620 colorectal carcinoma cell line which is *CDKN1A* defective (Supplementary Figure S4) decreased the infection rate of M1 virus and attenuated the subsequent cell killing of M1 (Figure 4L-4N). In summary, these loss- and gain-of-function experiments demonstrated that *CDKN1A* is the key IRG that is suppressed by RAS/RAF/MEK signaling to promote the replication of M1 virus.

CDKN1A is a tumor suppressor that mainly functions as a cell cycle checkpoint by binding to CDK1, CDK2 or the CDK4/6 complex [35]. We investigated whether the cell cycle plays an important role in the replication of M1 virus by inhibiting the activity of cyclin-dependent kinase 2 (CDK2), a primary factor mediating the cell cycle inhibition activity of *CDKN1A*.

K03861, an inhibitor of CDK2, modestly but significantly decreased the infection rate of M1 virus in a concentration-dependent manner in HCT-15 and MIA PaCa-2 cell lines (Figure 5A-5B), and titer of M1 virus was subsequently significantly inhibited by K03861 in these cell lines (Figure 5C-5D), phase contrast and fluorescence imaging also showed the inhibition of M1 viral infection by K03861 (Figure 5E). The results indicate that CDKN1A inhibits the replication of M1 virus by suppressing the cell cycle.

Knockdown of CDKN1A enhances the oncolytic effect of M1 virus *in vivo*

To further validate whether the suppression of CDKN1A enhances the oncolytic effect of M1 virus *in vivo*, we established an HCT-15 subcutaneous xenograft model in nude mice. HCT-15-negative control (NC) cells and HCT-15-shCDKN1A cells were implanted in the left and right hind flanks of mice, and M1 virus was injected through the caudal vein (Figure 6A). Compared with that of HCT-15-NC tumors, the growth of HCT-15-shCDKN1A tumors treated with M1 virus was modestly but significantly inhibited (Figure 6B), and the tumor size in the HCT-15-shCDKN1A group treated with M1 virus was smaller than that in the other three groups (Figure 6C). Consistent with the cellular results, M1 viral copy number in HCT-15-shCDKN1A tumors was increased compared with HCT-15-NC tumors (Figure 6D). Furthermore, immunohistochemical (IHC) staining was performed on tumor tissues to detect the expression of Ki-67 and cleaved caspase-3 (Cl-casp3) to measure the proliferation and apoptosis of tumor cells. We observed that Ki-67 expression was significantly downregulated and Cl-casp3 expression was coordinately upregulated in the M1 virus-treated HCT-15-shCDKN1A tumors (Figure 6E and 6F). These results further support the hypothesis that CDKN1A acts as an antiviral factor to inhibit the oncolytic effect of M1 virus *in vivo*.

CDKN1A deficiency is a biomarker for M1 therapy

The above CDKN1A loss- and gain-of-function experiments indicated that M1 may specifically target cancer cells deficient in CDKN1A. Therefore, we detected the protein

expression of CDKN1A in pancreatic carcinoma and colorectal carcinoma cell lines, which have been reported to frequently harbor *K-RAS* mutations, and analyzed the correlation between the cell-killing effect of M1 virus and CDKN1A expression. In both pancreatic and colorectal cancer cell lines, there is a significant negative correlation between CDKN1A expression and the killing capacity of M1 virus, which means that the lower the protein expression of CDKN1A is, the greater the cell-killing effect of M1 virus (Figure 7A and 7B, the protein expression and cell-killing effect of M1 are shown in Supplementary Figure S4 and Table S6). Furthermore, the relationship between the oncolytic effect of M1 and the expression of CDKN1A was also analyzed in 44 tumor cell lines, and CDKN1A expression was measured via reversed-phase protein array (RPPA) in the CCLE database. The expression of CDKN1A negatively correlated with the oncolytic effect of M1 in 44 tumor cell lines (Figure 7C, Supplementary Table S7). These results suggest that the protein expression of CDKN1A might predict the killing effect of M1 virus.

To elucidate the potential of M1 virus personalized therapy by detecting CDKN1A deficiency, we compared the expression of CDKN1A in both tumor and adjacent non-neoplastic tissue specimens from 38 colon cancer patients in the TCGA database [36]. The expression of CDKN1A in tumor tissues was lower than that in adjacent non-neoplastic tissues in over 90% (35/38) of patients (Figure 7D). Furthermore, we performed IHC on 2 tissue microarrays (TMAs) containing paired tumor and adjacent non-neoplastic clinical specimens from 143 colon cancer patients. CDKN1A expression was represented by the mean staining intensity, calculated by ImageScope software (Aperio). The expression of CDKN1A in tumor tissues was lower than that in adjacent non-neoplastic tissues in 58% (83/143) of patients (**Figure 7E and 7F**). Both the database and our experiments strongly suggest that the expression of CDKN1A was frequently deficient in colorectal cancers, which implies the application of M1 virus.

Discussion

In this paper, we report that the oncogenic RAS/RAF/MEK pathway promotes the replication and oncolytic effect of M1 virus by inhibiting the expression of the key antiviral factor CDKN1A. More importantly, cancer cell lines with lower expression levels of CDKN1A showed greater sensitivity to M1 virus than those with higher levels, and the deficiency of CDKN1A is a ubiquitous event in colorectal cancer patients. Our data suggest that CDKN1A is a suitable biomarker for M1 virus therapy. Our report provides a candidate research program and working model to screen and identify oncogenic pathways as well as biomarkers that other oncolytic viruses utilize to facilitate their replication.

Despite more than three decades of intensive effort, no effective pharmacologic inhibitors of the RAS oncoproteins have reached the clinic, promoting the widely held perception that RAS proteins are “undruggable” [37]. According to our results, M1 virus might offer a renewed hope for the treatment of cancer with abnormal *RAS* activation, making *RAS*-driven tumors “druggable”. Among all cancer-driven genes, *RAS* is the most frequently mutated oncogene family in human cancers. The top four cancer types harbor *RAS* mutation including pancreatic ductal adenocarcinoma (97.7%), colorectal adenocarcinoma (52.2%), multiple myeloma (42.6%) and lung adenocarcinoma (32.2%) [37]. The high percentage of *RAS* mutation in tumors indicates that M1 virus might be effective in a large proportion of cancer patients.

The hypothesis that oncolytic viruses exploit the deficiencies of antiviral pathways and oncogenic signaling between tumor and normal cells to selectively target and kill cancer cells has been strongly proven. The RAS pathway is a typical oncogenic pathway reported to facilitate the replication of various oncolytic viruses. However, to date, no clinical trials have validated *RAS* mutations as a biomarker for any oncolytic virus, which may be due to the upregulation of other compensatory pathways downstream of RAS that control the expression of antiviral genes in patients; thus, identifying the antiviral genes regulated by

the RAS pathway as biomarkers for oncolytic viruses is urgently required. The expression of components of the interferon pathway, such as PKR and IRF1, has been reported to be downregulated by the RAS pathway. However, the expression of these genes has not been proven to be substantially decreased in tumors. Here, we found that a new antiviral gene, CDKN1A, downstream of the RAS pathway to suppress the replication and oncolytic effect of M1 virus, and it has been reported to be a tumor suppressor. Our data clearly support the hypothesis that deficiency in both tumor suppressor and antiviral pathways support the tumor selection mechanism of oncolytic viruses and provide a new biomarker for accurate oncolytic viro-therapy.

CDKN1A is a universal cell cycle inhibitor directly controlled by p53 and p53-independent pathways, and the loss of CDKN1A causes carcinogenesis by inducing growth arrest, regulating the expression of genes associated with senescence, and protecting cells from apoptosis [34, 35, 38]. Consistently, our data prove that CDKN1A expression is consistently deficient in colon cancer, further supporting the reports that CDKN1A is a tumor suppressor. In this study, we demonstrate that CDKN1A inhibits the replication of M1, whereas the inhibition of CDKN1A promotes the replication and oncolytic effect of M1 virus. In tumors with low CDKN1A expression, the oncolytic effect of M1 virus is stronger than that in tumors with high CDKN1A expression. We hypothesize that CDKN1A controls the cell cycle, but viral replication needs increased amounts of material and energy, so in cancer cells without CDKN1A to control proliferation, the proliferation rate increases and provides sufficient cellular resources for the synthesis and assembly of new viral particles.

Genetic heterogeneity represents one of the most significant hallmarks of cancer, indicating that universal treatment for all patients is problematic and that personalized medicine is required for cancer therapy. The discovery of biomarkers in tumors provides a potential strategy to solve this problem [39]. The detection of biomarkers before treatment with an anticancer drug decreases the chance of a patient receiving an ineffective

medication and largely increases the efficiency of the drug. In 2017, the PD-1 antibody pembrolizumab was approved by the FDA for patients with microsatellite instability-high (MSI-H) and deficient mismatch repair (dMMR) [40]. It is the first anticancer strategy that is distinguished by a biomarker but not the organ origin of the tumor. In this study, we found that the oncolytic effect of M1 virus negatively correlated with the expression of CDKN1A in tumor cells. CDKN1A serves as a tumor suppressor and is deficient in various cancer types in addition to colorectal carcinoma [41], which indicates that CDKN1A expression may serve as an M1 virus biomarker in pan-cancer types.

Sorafenib is the first oral multikinase inhibitor that targets RAF. It was first approved by the FDA for the treatment of advanced renal cell carcinoma in 2005 [31]. Subsequently, it was approved for other indications, including hepatocellular carcinoma and radioactive iodine-refractory differentiated thyroid cancer [42]. We have previously reported that M1 virus has a natural tropism for hepatocellular carcinoma and multiple kinds of cancers [23]. Moreover, we have identified various anticancer chemicals in clinical use or in the clinical trial stage, such as VCP inhibitors [27], DNK-PK inhibitors [28], Smac mimetics [24], and Bcl-XL inhibitors [26], can sensitize tumors to M1 virus. Here, we report that sorafenib inhibits the replication and oncolytic effect of M1 virus. These results suggest that in the future, the combination of M1 virus and sorafenib should be avoided in the clinic.

Conclusions

In summary, our research shows that tumors involving RAS signaling harbor a natural vulnerability to oncolytic M1 virus and illustrate that CDKN1A is the key downstream antiviral factor to predict the oncolytic efficacy of M1 virus.

Data accessibility. The microarray data was submitted to the Gene Expression Omnibus (GEO) (<https://www.ncbi.nlm.nih.gov/geo/>). The accession number is GSE134487.

Author contributions

J.C., J.K.L., and G.M.Y. contributed to the experimental design and data analysis. J.C., J.K.L. and M.S. contributed to manuscript writing and editing. X.C.L. contributed to the data analysis of the expression profile data. K.Y.L., W.C., L.G., J.F.Z., W.C.X., Z.Q.L. and C.W.H. contributed to the cellular and animal experiments. Y.L. contributed to the IHC experiments and IHC data analysis. W.B.Z. and J.H. contributed to the animal experiments.

Acknowledgments and funding sources

This work was supported by grants from the National Natural Science Foundation of China (No. 81703537, No. 81673447), China Postdoctoral Science Foundation Project (2018M640875), Fundamental Research Funds for the Central Universities (No. 19ykpy166), Leading team for entrepreneurship in Guangzhou, Guangdong Province (No. 201809020004), the National Major Scientific and Technological Special Project for “Significant New Drugs Development” during the 13th Five-Year Plan Period (No. 2018ZX09733002), and Guangzhou People's Livelihood Science and Technology Tackling Key Projects (201803010113).

Disclosure of conflicts of interest

J.F.Z., W.C.X., Z.Q.L., and M.S. are employees of Guangzhou Virotech Pharmaceutical Co., Ltd. (GVP) and performed the cellular and animal experiments. The present research is not funded by GVP. The authors declare that there are no potential conflicts of interest.

Figure legends

Figure 1. Tumor cells harboring mutations in *KRAS* were more sensitive to M1 virus than those not harboring mutations in *KRAS*.

(A) Volcano plot showing the relationship between the oncolytic effect of M1 virus and

oncogenic mutations in 52 tumor cell lines. The X-axis shows the log fold change of the oncolytic effect (represented by EC50 values) in *KRAS* mutant cells versus *KRAS* wild type cells. The EC50 values of M1 was analyzed as below: 52 tumor cell lines were treated with different MOI of M1 virus (0, 0.001, 0.1, 1, 10 and 100 (100 MOI for resistant cell lines such as HCC827, HEL, ME180, Reh and SiHa)) for 48 hours, the cell killing percentage was detected by MTT. The dose response curve of multi-MOI of M1 virus was fitted with nonlinear regression in each cell line, and EC50 (viral dose to kill 50% cancer cells) was calculated. The Y-axis shows the log₁₀ *p* values analyzed by the chi-square test; n=3.

(B) Violin figure showing the EC50 of M1 virus in *K-RAS* wild type and mutant cancer cells; n=3. MUT: mutation. Statistical analysis was performed by two-tailed Student's *t* test.

(C-D) The HCT-15 and MIA PaCa-2 cell lines were treated with siRNAs targeting K-RAS for 48 hours, M1 virus (MOI=1 pfu/cell) was added for another 60 hours, and the viability was detected by MTT; n=3. Statistical analysis was performed by one-way ANOVA with Dunnett's test for pairwise comparisons.

(E-I) The HCT-15 and MIA PaCa-2 cell lines were treated with siRNAs targeting K-RAS for 48 hours, M1 virus (MOI=1 pfu/cell) was added for another 24 hours, and the infection rate of M1 virus (GFP percentage) was detected by flow cytometry (E-F). Phase contrast and fluorescence pictures are shown (G). Titer of M1 virus was detected by TCID50 method (H-I). n=3. Statistical analysis was performed by one-way ANOVA with Dunnett's test for pairwise comparisons. The pictures show one representative result from three similar experimental replicates. Scale bar, 100 μm.

Error bars represent the mean ± SD obtained from three independent experiments.

p*<0.05, ** *p*<0.01, * *p*<0.001.

See also in Supplementary Figure 1, Table S1 and Table S2. For TCID50 assay, the starting cell numbers of compared group are the same.

Figure 2. Sorafenib and U0126 inhibited the oncolytic effect and replication of M1 virus.

(A-D) HCT-15 and MIA PaCa-2 cell lines were treated with different concentrations of sorafenib or U0126 with or without M1 (MOI=1 pfu/cell) for 60 hours, and cell viability was detected by MTT; n=3. Statistical analysis was performed by one-way ANOVA with Dunnett's test for pairwise comparisons. (E-F) HCT-15 and MIA PaCa-2 cell lines were treated with control, M1 (MOI=1 pfu/cell), U0126 (16 μ M) or M1 (MOI=1 pfu/cell) plus U0126 (16 μ M) for 24 hours, and phase contrast and fluorescence pictures are shown. The results show one representative result from three similar experimental replicates. Scale bar, 100 μ m.

(G-H) HCT-15 and MIA PaCa-2 cells were treated with M1 (MOI=1 pfu/cell) and M1 (MOI=1 pfu/cell) plus U0126 (16 μ M) for 24 hours, and the infection rate of M1 virus (GFP percentage) was detected by flow cytometry; n=3. Statistical analysis was performed by two-tailed Student's *t* test.

(I-J) HCT-15 and MIA PaCa-2 cells were treated with control, M1 (MOI=1 pfu/cell), U0126 (16 μ M) or M1 (MOI=1 pfu/cell) plus U0126 (16 μ M) for the indicated times, and the levels of E1, NS3 and p-ERK were detected by western blot. The results show one representative result from three similar experimental replicates.

Error bars represent the mean \pm SD obtained from three independent experiments. *n.s.*, not significant; **p*<0.05, ** *p*<0.01, *** *p*<0.001. See also in Supplementary Figure 2.

Figure 3. U0126 inhibited RAS signaling and upregulated the expression of antiviral genes.

(A-C) GSEA of the RAS-regulated gene set (A), interferon alpha response gene set (B) and interferon beta gene set (C) after M1 (MOI=1 pfu/cell) and M1 (MOI=1 pfu/cell) plus U0126 (16 μ M) treatment of the HCT-15 cell line for 24 hours. Values of NES, *p* and FDR are shown in each box.

(D) The heatmap of the top 20 IRGs upregulated in the U0126 plus M1-treated HCT 15

cells compared with M1 (MU/M) treated HCT 15 cells is shown.

(E-F) The HCT-15 cell line was treated with control, M1 (MOI=1 pfu/cell), U0126 (16 μ M) or M1 (MOI=1 pfu/cell) plus U0126 (16 μ M) for 24 hours, and the relative expression of the top 10 IRGs (including *IFIT3*, *CDKN1A*, *MX2*, *IFI27*, *ID1*, *CYP1B1*, *ATP10D*, *PNRC1*, *JUN*, and *DDIT4*) in (D) was detected by Q-PCR; n=3. Statistical analysis was performed by one-way ANOVA with Dunnett's test for pairwise comparisons.

(D) Summary of the top 10 IRGs treated with U0126 plus M1 compared with M1 (MU/M). Error bars represent the mean \pm SD obtained from three independent experiments. CTL, control; MU, M1+U0126. *n.s.*, not significant; * p <0.05, ** p <0.01, *** p <0.001. See also Supplementary Tables S3-S5.

Figure 4. CDKN1A was the key IRG that inhibited the replication of M1 virus.

(A) The HCT-15 cell line was treated with siRNAs targeting *IFIT3*, *CDKN1A*, *MX2*, *IFI27* and *ID1* for 48 hours, M1 virus (MOI=1 pfu/cell) was added for another 24 hours, and the infection rate of M1 virus (GFP percentage) was detected by flow cytometry; n=3. Statistical analysis was performed by one-way ANOVA with Dunnett's test for pairwise comparisons.

(B) The knockdown efficiency of siRNAs (48 hours) targeting *CDKN1A* in MIA PaCa-2 and PANC-1 cell lines detected by western blot.

(C-F) MIA PaCa-2 and PANC-1 cell lines were treated with siRNAs against *CDKN1A* for 48 hours, M1 virus (MOI=1 pfu/cell) was added for another 24 hours, and the infection rate

(C-D) and titer (E-F) of M1 virus were detected by flow cytometry and the TCID₅₀; n=3. Statistical analysis was performed by one-way ANOVA with Dunnett's test for pairwise comparisons.

(G-I) The infection rate and titer of M1 virus in HCT-15 and PANC-1 cell lines treated with or without sh*CDKN1A* were detected by flow cytometry and the TCID₅₀. The efficiency of sh*CDKN1A* was detected by western blot; n=3. Statistical analysis was performed by two-tailed Student's *t* test.

(J-K) The infection rates and titers of M1 virus in the HCT-15 cells treated with or without CDKN1A were detected by flow cytometry and the TCID50. The overexpression of CDKN1A by lentivirus was detected by western blot; n=3. Statistical analysis was performed by two-tailed Student's *t* test.

(L) SW620 cell line was transfected by CDKN1A vector or control vector, the overexpression of CDKN1A was verified by western blot.

(M-N) SW620 cells transfected with or without CDKN1A vector were treated with M1 virus (MOI=1 pfu/cell) for 24 hours, infection rate of M1 was detected by flow cytometry (M). 60 hours later, cell viability was detected by MTT method (N). n=3. Statistical analysis was performed by two-tailed Student's *t* test.

Error bars represent the mean \pm SD obtained from three independent experiments. *n.s.*, not significant; **p*<0.05, ** *p*<0.01, *** *p*<0.001. See also Supplementary Figure S3 and S4. For TCID50 assay, the starting cell numbers of compared group are the same.

Figure 5. The CDK2 inhibitor K03861 inhibited the replication of M1 virus.

(A-E) HCT-15 and MIA PaCa-2 cells were treated with different concentrations of K03861 with or without M1 virus (MOI=1 pfu/cell) for 24 hours; then, the infection rate (A and B) was detected by flow cytometry, the titer was detected by TCID50 (C and D), phase contrast and fluorescence pictures were taken (E). Statistical analysis was performed by two-tailed Student's *t* test or one-way ANOVA with Dunnett's test for pairwise comparisons.

Error bars represent the mean \pm SD obtained from three independent experiments. *n.s.*, not significant; **p*<0.05, ** *p*<0.01, *** *p*<0.001. For TCID50 assay, the starting cell numbers of compared group are the same.

Figure 6. Knockdown of CDKN1A by shRNA enhanced the oncolytic effect of M1 virus in HCT-15 xenograft tumors.

(A) Schematic of the *in vivo* experiment. In brief, HCT-15-NC and HCT-15-shCDKN1A

cells were inoculated in each hind flank of the nude mice. Six days later, tumors were visible, and M1 virus was injected intravenously for 14 days. Tumors were measured every other day, and the tumor volume was calculated by the formula $(\text{length} \times \text{width}^2)/2$.

(B) Growth curve of the tumors in each group; $n=7$. Error bars represent the mean \pm SEM. Statistical analysis was performed by two-tailed paired Student's *t* test.

(C) At the endpoint, mice were anesthetized and sacrificed, and tumors were subsequently dissected and photographed.

(D) 3 days after the first medication, total RNA in tumors was extracted and viral copy numbers were detected by Taqman qRT-PCR. $n=3$, Statistical analysis was performed by two-tailed paired Student's *t* test.

(E) At the endpoint, the expression of cleaved caspase-3 and Ki-67 in tumors was detected by IHC. Scale bars, 100 μm .

(F), Statistical analysis of Ki-67 and cleaved caspase-3 IHC intensity; $n=3$, Error bars represent the mean \pm SD. Statistical analysis was performed by two-tailed paired Student's *t* test.

n.s., not significant; * $p<0.05$, ** $p<0.01$, *** $p<0.001$.

Figure 7. Expression of CDKN1A negatively correlated with the oncolytic effect of M1 virus and served as a biomarker for M1.

(A-B) The correlation between the oncolytic effect of M1 virus and the protein expression of CDKN1A in colorectal cancer cell lines (A) and pancreatic cancer cell lines (B). The protein level of CDKN1A was detected by western blot (Supplementary Figure S4), and the oncolytic effect of M1 virus is shown in Supplementary Table 6. Statistical analysis was performed by the Pearson correlation test.

(C) The correlation between the oncolytic effect of M1 virus and protein expression of CDKN1A in 44 tumor cell lines. The oncolytic effect of M1 was indicated by the cell-killing percentage in the 44 tumor cell lines treated with M1 virus (MOI=10 pfu/cell) for 48 hours and detected by MTT; $n=3$. The X-axis shows the protein expression of CDKN1A

measured by reversed-phase protein array (RPPA) in the CCLE data. Statistical analysis was performed by the Pearson correlation test.

(D) HTSeq count showing the mRNA expression of CDKN1A in tumor and adjacent non-neoplastic tissue from colon cancer patients in the TCGA data, the percentage of patients showing lower expression of CDKN1A in tumor tissue than that in adjacent non-neoplastic tissue was calculated. Blue dots represent tumor tissues, red dots represent paired adjacent non-neoplastic tissues, black lines connect paired tumor and adjacent non-neoplastic tissue from the same patient. $n=38$. Statistical analysis was performed by two-tailed paired Student's *t* test.

(E) IHC staining intensity of CDKN1A expression in tissue microarrays containing paired tumor and adjacent non-neoplastic clinical specimens from 143 colon cancer patients. The IHC level is presented as the mean staining intensity calculated using ImageScope software (Aperio), the percentage of patients showing lower expression of CDKN1A in tumor tissue than that in adjacent non-neoplastic tissue was calculated. Statistical analysis was performed by two-tailed paired Student's *t* test.

(F) Representative pictures of the IHC in (E). Scale bars, 50 μm .

* $p<0.05$, ** $p<0.01$, *** $p<0.001$. See also Supplementary Figure S4 and Tables S6 and S7.

References

1. Russell, S.J., K.W. Peng, and J.C. Bell (2012) Oncolytic virotherapy. *Nat Biotechnol* 30(7), 658-70.
2. Parato, K.A., D. Senger, P.A. Forsyth, and J.C. Bell (2005) Recent progress in the battle between oncolytic viruses and tumours. *Nat Rev Cancer* 5(12), 965-76.
3. Lawler, S.E., M.C. Speranza, C.F. Cho, and E.A. Chiocca (2017) Oncolytic Viruses in Cancer Treatment: A Review. *JAMA Oncol* 3(6), 841-849.

-
4. de Grujil, T.D., A.B. Janssen, and V.W. van Beusechem (2015) Arming oncolytic viruses to leverage antitumor immunity. *Expert Opin Biol Ther* 15(7), 959-71.
5. Russell, S.J. and K.W. Peng (2007) Viruses as anticancer drugs. *Trends Pharmacol Sci* 28(7), 326-33.
6. Bommareddy, P.K., M. Shettigar, and H.L. Kaufman (2018) Integrating oncolytic viruses in combination cancer immunotherapy. *Nat Rev Immunol* 18(8), 498-513.
7. Kaufman, H.L., F.J. Kohlhapp, and A. Zloza (2015) Oncolytic viruses: a new class of immunotherapy drugs. *Nat Rev Drug Discov* 14(9), 642-62.
8. Twumasi-Boateng, K., J.L. Pettigrew, Y.Y.E. Kwok, J.C. Bell, and B.H. Nelson (2018) Oncolytic viruses as engineering platforms for combination immunotherapy. *Nat Rev Cancer* 18(7), 419-432.
9. Andtbacka, R.H., H.L. Kaufman, F. Collichio, T. Amatruda, N. Senzer, J. Chesney, et al. (2015) Talimogene Laherparepvec Improves Durable Response Rate in Patients With Advanced Melanoma. *J Clin Oncol* 33(25), 2780-8.
10. Martinez-Quintanilla, J., I. Seah, M. Chua, and K. Shah (2019) Oncolytic viruses: overcoming translational challenges. *J Clin Invest* 130, 1407-1418.
11. Pikor, L.A., J.C. Bell, and J.S. Diallo (2015) Oncolytic Viruses: Exploiting Cancer's Deal with the Devil. *Trends Cancer* 1(4), 266-277.
12. Mansour, M., P. Palese, and D. Zamarin (2011) Oncolytic specificity of Newcastle disease virus is mediated by selectivity for apoptosis-resistant cells. *J Virol* 85(12), 6015-23.
13. Teferi, W.M., K. Dodd, R. Maranchuk, N. Favis, and D.H. Evans (2013) A whole-genome RNA interference screen for human cell factors affecting myxoma

virus replication. *J Virol* 87(8), 4623-41.

14. Baril, M., S. Es-Saad, L. Chatel-Chaix, K. Fink, T. Pham, V.A. Raymond, et al. (2013) Genome-wide RNAi screen reveals a new role of a WNT/CTNNB1 signaling pathway as negative regulator of virus-induced innate immune responses. *PLoS Pathog* 9(6), e1003416.
15. Shapira, S.D., I. Gat-Viks, B.O. Shum, A. Dricot, M.M. de Grace, L. Wu, et al. (2009) A physical and regulatory map of host-influenza interactions reveals pathways in H1N1 infection. *Cell* 139(7), 1255-67.
16. Strong, J.E., M.C. Coffey, D. Tang, P. Sabinin, and P.W. Lee (1998) The molecular basis of viral oncolysis: usurpation of the Ras signaling pathway by reovirus. *EMBO J* 17(12), 3351-62.
17. Parato, K.A., C.J. Breitbach, F. Le Boeuf, J. Wang, C. Storbeck, C. Ilkow, et al. (2012) The oncolytic poxvirus JX-594 selectively replicates in and destroys cancer cells driven by genetic pathways commonly activated in cancers. *Mol Ther* 20(4), 749-58.
18. Farassati, F., A.D. Yang, and P.W. Lee (2001) Oncogenes in Ras signalling pathway dictate host-cell permissiveness to herpes simplex virus 1. *Nat Cell Biol* 3(8), 745-50.
19. Cuddington, B.P. and K.L. Mossman (2014) Permissiveness of human cancer cells to oncolytic bovine herpesvirus 1 is mediated in part by KRAS activity. *J Virol* 88(12), 6885-95.
20. Zhai, Y.G., H.Y. Wang, X.H. Sun, S.H. Fu, H.Q. Wang, H. Attoui, Q. Tang, and G.D. Liang (2008) Complete sequence characterization of isolates of Getah virus (genus Alphavirus, family Togaviridae) from China. *J Gen Virol* 89(Pt 6), 1446-56.

21. Hu, J., X.F. Cai, and G. Yan (2009) Alphavirus M1 induces apoptosis of malignant glioma cells via downregulation and nucleolar translocation of p21WAF1/CIP1 protein. *Cell Cycle* 8(20), 3328-39.
22. Zhang, H., Y. Lin, K. Li, J. Liang, X. Xiao, J. Cai, et al. (2016) Naturally Existing Oncolytic Virus M1 Is Nonpathogenic for the Nonhuman Primates After Multiple Rounds of Repeated Intravenous Injections. *Hum Gene Ther* 27(9), 700-11.
23. Lin, Y., H. Zhang, J. Liang, K. Li, W. Zhu, L. Fu, et al. (2014) Identification and characterization of alphavirus M1 as a selective oncolytic virus targeting ZAP-defective human cancers. *Proc Natl Acad Sci U S A* 111(42), E4504-12.
24. Cai, J., Y. Lin, H. Zhang, J. Liang, Y. Tan, W.K. Cavenee, and G. Yan (2017) Selective replication of oncolytic virus M1 results in a bystander killing effect that is potentiated by Smac mimetics. *Proc Natl Acad Sci U S A* 114(26), 6812-6817.
25. Li, K., H. Zhang, J. Qiu, Y. Lin, J. Liang, X. Xiao, et al. (2016) Activation of Cyclic Adenosine Monophosphate Pathway Increases the Sensitivity of Cancer Cells to the Oncolytic Virus M1. *Mol Ther* 24(1), 156-65.
26. Tan, Y., Y. Lin, K. Li, X. Xiao, J. Liang, J. Cai, et al. (2017) Selective Antagonism of Bcl-xL Potentiates M1 Oncolysis by Enhancing Mitochondrial Apoptosis. *Hum Gene Ther*.
27. Zhang, H., K. Li, Y. Lin, F. Xing, X. Xiao, J. Cai, et al. (2017) Targeting VCP enhances anticancer activity of oncolytic virus M1 in hepatocellular carcinoma. *Sci Transl Med* 9(404), eaam7996.
28. Xiao, X., J. Liang, C. Huang, K. Li, F. Xing, W. Zhu, et al. (2018) DNA-PK inhibition synergizes with oncolytic virus M1 by inhibiting antiviral response and potentiating DNA damage. *Nat Commun* 9(1), 4342.

29. Liang, J., L. Guo, K. Li, X. Xiao, W. Zhu, X. Zheng, et al. (2018) Inhibition of the mevalonate pathway enhances cancer cell oncolysis mediated by M1 virus. *Nat Commun* 9(1), 1524.
30. Ghandi, M., F.W. Huang, J. Jane-Valbuena, G.V. Kryukov, C.C. Lo, E.R. McDonald, 3rd, et al. (2019) Next-generation characterization of the Cancer Cell Line Encyclopedia. *Nature* 569(7757), 503-508.
31. Wilhelm, S., C. Carter, M. Lynch, T. Lowinger, J. Dumas, R.A. Smith, B. Schwartz, R. Simantov, and S. Kelley (2006) Discovery and development of sorafenib: a multikinase inhibitor for treating cancer. *Nat Rev Drug Discov* 5(10), 835-44.
32. Duncia, J.V., J.B. Santella, 3rd, C.A. Higley, W.J. Pitts, J. Wityak, W.E. Fietze, et al. (1998) MEK inhibitors: the chemistry and biological activity of U0126, its analogs, and cyclization products. *Bioorg Med Chem Lett* 8(20), 2839-44.
33. Sadler, A.J. and B.R. Williams (2008) Interferon-inducible antiviral effectors. *Nat Rev Immunol* 8(7), 559-68.
34. El-Deiry, W.S. (2016) p21(WAF1) Mediates Cell-Cycle Inhibition, Relevant to Cancer Suppression and Therapy. *Cancer Res* 76(18), 5189-91.
35. Abbas, T. and A. Dutta (2009) p21 in cancer: intricate networks and multiple activities. *Nat Rev Cancer* 9(6), 400-14.
36. Cancer Genome Atlas, N. (2012) Comprehensive molecular characterization of human colon and rectal cancer. *Nature* 487(7407), 330-7.
37. Cox, A.D., S.W. Fesik, A.C. Kimmelman, J. Luo, and C.J. Der (2014) Drugging the undruggable RAS: Mission possible? *Nat Rev Drug Discov* 13(11), 828-51.
38. Georgakilas, A.G., O.A. Martin, and W.M. Bonner (2017) p21: A Two-Faced

Genome Guardian. Trends Mol Med 23(4), 310-319.

39. Ludwig, J.A. and J.N. Weinstein (2005) Biomarkers in Cancer Staging, Prognosis and Treatment Selection. Nat Rev Cancer 5, 845-856.
40. Administration, U.S.F.a.D. (2017) FDA approves first cancer treatment for any solid tumor with a specific genetic feature.
41. Shamloo, B. and S. Usluer (2019) p21 in Cancer Research. Cancers (Basel) 11(8).
42. Mattina, J., B. Carlisle, Y. Hachem, D. Fergusson, and J. Kimmelman (2017) Inefficiencies and Patient Burdens in the Development of the Targeted Cancer Drug Sorafenib: A Systematic Review. PLoS Biol 15(2), e2000487.

Supporting Information

Table S1. Oncolytic effect of M1 virus and status in *k-Ras* in 52 tumor cells. Refers to Figure 1.

Table S2. The mutation status of whole genome in 52 tumor cells. Refers to Figure 1.

Figure S1. The efficiency of siRNAs to *K-RAS*.

Figure S2. Cobimetinib and Trametinib inhibited the oncolytic effect and replication of M1 virus.

Table S3. Genes regulated by *k-Ras* activation in expression profile database. Refers to Figure 3.

Table S4. Interferon alpha response genes in expression profile database. Refers to Figure 3.

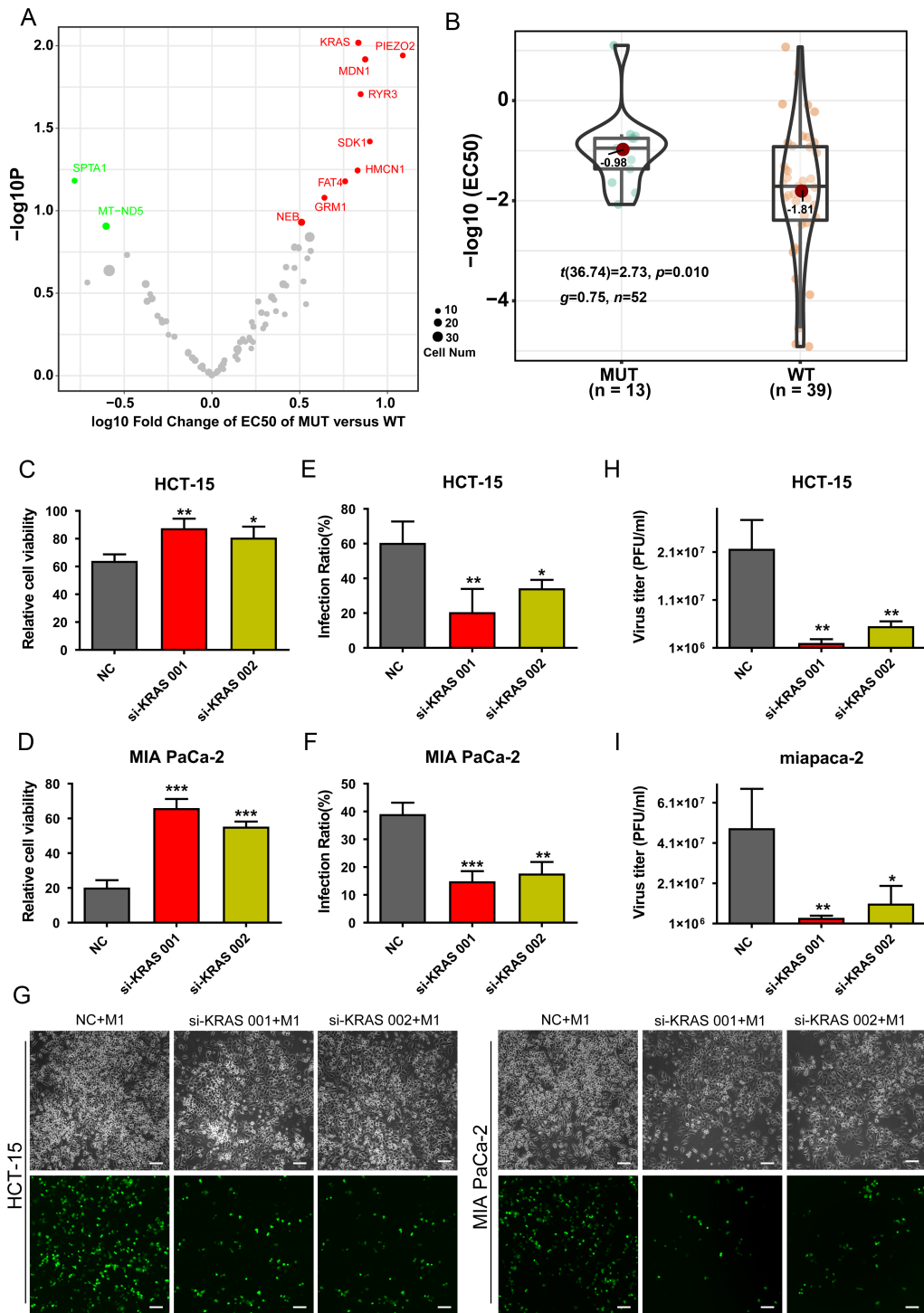
Table S5. Interferon beta response genes in expression profile database. Refers to Figure 3.

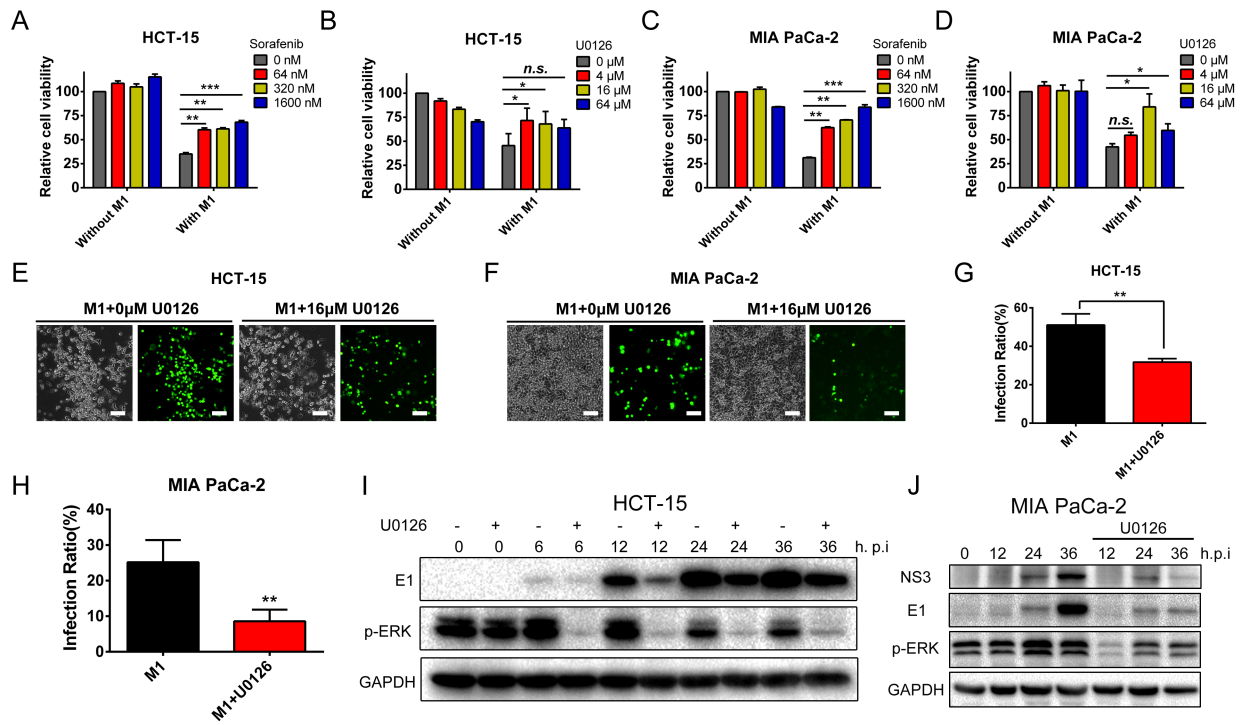
Figure S3. The efficiency of siRNAs. Refers to Figure 4.

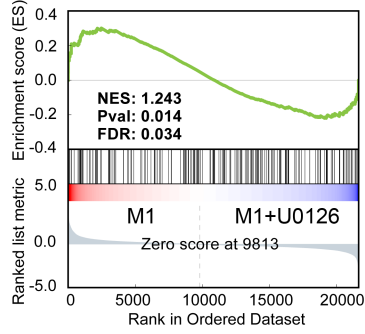
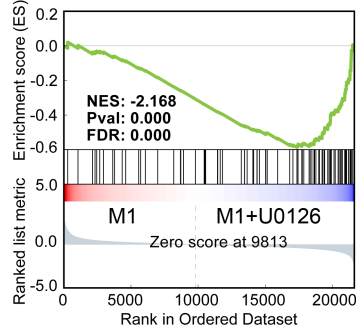
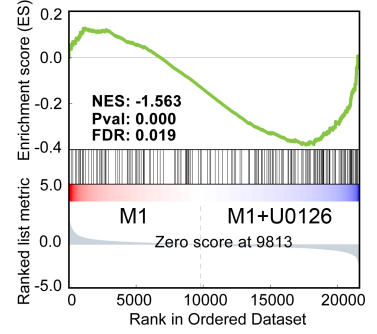
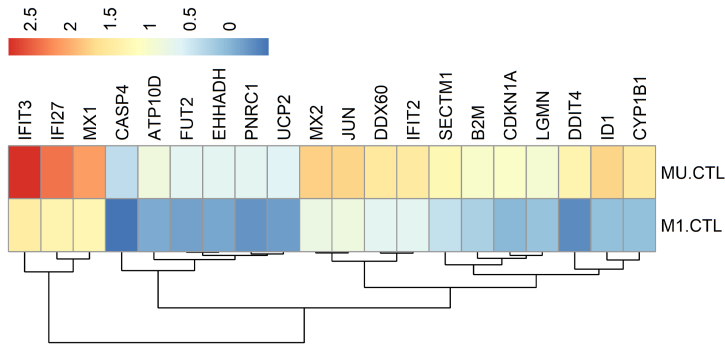
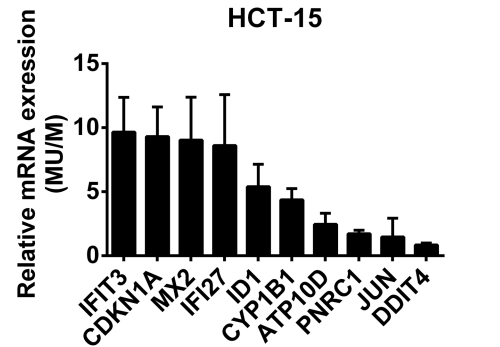
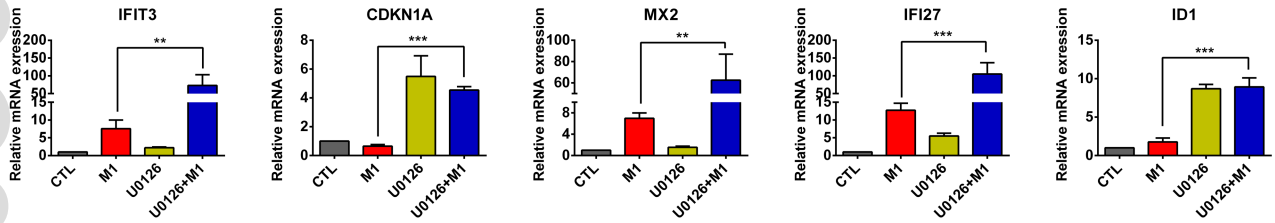
Figure S4. Protein level of CDKN1A. Refers to Figure 7.

Table S6. Oncolytic effect of M1 virus in colon cancer cell lines and pancreatic cancer cell lines. Refers to Figure 7.

Table S7. Oncolytic effect of M1 virus and the protein expression of CDKN1A in 44 tumor cells. Refers to Figure 7.





A Genes regulated by k-Ras activation**B** Interferon alpha response**C** Interferon beta response**D****G****E****F**